

## KINETICS OF OIL SHALE PYROLYSIS IN AN AUTOCLAVE UNDER NON-LINEAR INCREASE OF TEMPERATURE

I. JOHANNES<sup>\*</sup>, L. TIIKMA

Institute of Oil Shale Research,  
Tallinn University of Technology  
17 Akadeemia Rd., Tallinn, 12618, Estonia

*An approximate step-by-step model has been deduced for description of the thermal decomposition kinetics of Estonian oil shale in an autoclave under non-linear increase of temperature. The apparent first-order kinetic constants have been estimated for the overall parallel formation of gaseous and liquid phases from the initial organic matter, for the parallel and consequent formation of gas from the liquid product at the stage of oil shale thermal decomposition, and for the parallel formation of gas and solid residue from the liquid product in the cracking stage. A linear dependence between the apparent Arrhenius constants  $\ln A = 0.179E - 3.258$  ( $n = 24$ ,  $r = 0.991$ ) was revealed for different kinetic steps of kukersite pyrolysis using the constants estimated in this work and published by others.*

### Introduction

The pyrolysis of oil shale is a very complex process involving the parallel and consequent rupture of different chemical bonds with different energies. Therefore, approximate models have been proposed for decomposition kinetics of oil shales. At that, the different nature of kerogen obtained from different geographical sites has caused variation in oil generation from the oil shales. Furthermore, the different equipments applied for investigations have affected the apparent kinetic constants found.

Considerable research work has been made to understand the mechanism and kinetics of the thermal decomposition of Baltic oil shale (kukersite) in the middle of the last century [1–7]. Among the somewhat controversial pyrolysis schemes proposed, the most comprehensive one was worked out by Aarna [2–4, 6]. This scheme rejects the homogeneous composition of shale oil assumed by Hissin [1] and proves that evolution of decomposition water, CO<sub>2</sub> and H<sub>2</sub>S begins at 170–180 °C. Typical to kukersite slow (during

---

<sup>\*</sup> Corresponding author: e-mail [ille.johannes@ttu.ee](mailto:ille.johannes@ttu.ee)

744 hours at 300 °C and 14 hours at 330 °C [2]) parallel formation of oil light fractions and thermobitumen takes place at 250–350 °C. Thermobitumen is a high-molecular decomposition product of kerogen soluble in organic solvents and changing in time and temperature. The secondary decomposition of thermobitumen yielding heavier oil fractions, gas, water and solid residue (semicoke) begins at temperatures 325–350 °C.

Understandable that the kinetic models of kukersite pyrolysis based on the weight loss data cannot consider all the reaction steps, especially rearrangements in thermobitumen. It was demonstrated [4, 6] that the apparent rate coefficients for the total decomposition of kukersite decreased significantly in time, in spite of the satisfactory linearity of the Arrhenius plot ( $\ln k - 1/T$ ) obtained at any definite pyrolysis prolongation. So, the adequate mathematical modeling of the complicated process was declared impossible in these years [7].

Later, in the eighties, Zakharov [8, 9] reported the results of non-isothermal decomposition ( $b = 20$  K/min) of Baltic oil shale. Contrary to the scheme above, oil formation began first at 315 °C; its maximum yield at 405–410 °C was followed at 410 °C by evolution of gases: CH<sub>4</sub> (350 °C), C<sub>n</sub>H<sub>m</sub> and H<sub>2</sub> with the corresponding maximums at 520, 450 and 540 °C. For mathematical description of the pyrolysis kinetics, the process was divided into two first-order kinetic stages – the overall oil formation and the parallel formation of the oil and the three gases monitored. For estimation of the kinetic constants, the apparent activation energy ( $E$ ) and pre-exponential factor ( $A$ ), the formal equation for the degree of kukersite decomposition

$$\alpha = 1 - \exp\{-AT/b \exp(-E/RT)[RT/E - 2(RT/E)^2]\} \quad (1)$$

was solved using the least squares method. The values of  $E$  and  $A$  found were for oil 134 kJ/mol and  $1.05E + 07$  s<sup>-1</sup>, and for the total volatiles – 178 kJ/mol and  $3.0E + 06$  s<sup>-1</sup>.

In the nineties of the last century Kundel [10] has studied pyrolysis of kukersite basing on the weight loss data obtained by thermogravimetric analysis (TGA). The apparent kinetic constants were calculated by the differential equation

$$d\alpha/dt = A/b \exp(-E/RT)(1 - \alpha)^n \quad (2)$$

where degree of decomposition

$$\alpha = (m_0 - m_t)/(m_0 - m_\infty) \quad (3)$$

and  $m_0$ ,  $m_\infty$  and  $m_t$  were the initial, final and current mass of kerogen.

It was established that analogous to the study [6],  $E$  increased from 160 to 200 kJ/mol when  $\alpha$  increased from 1 to 40%. Besides, the yield of volatiles increased non-linearly with increase of the kerogen percentage ( $OM = 20.9$ –

87.45%) and heating rate ( $b = 1.9\text{--}120$  K/min). A mathematical model for satisfactory prediction of  $\alpha$  was proposed. In the complicated model the values of  $E$  and  $A$  were calculated from the TGA data estimated at the maximum reaction rate ( $w_M$ ). The third-order regression equations *versus* double logarithms of  $b$  and  $OM$  were applied for  $w_M$ , and for the temperature ( $t_M$ ), yields of volatiles ( $V_M$ ) and remained kerogen ( $M_M$ ) at  $w_M$ .

Skala *et al.* [11] have constructed models for pyrolysis of Yugoslavian oil shales based on the single-, two- and multi-step reaction schemes using the data of TGA and differential scanning calorimetry (d.s.c.). The kinetic parameters of Alexinac oil shale decomposition,  $E$  and  $A$ , obtained by the integral single-step model using the heat absorption data from d.s.c. were 215 kJ/mol and  $9.76E + 14 \text{ min}^{-1}$ , i.e. 2–2.5 times lower compared with the data of TGA [12]. The multi-step model proposed consisted of twelve equations representing the parallel decomposition of two initial components, kerogen ( $K$ ) and bitumen ( $B$ ), into hypothetical volatilized products ( $P_1\text{--}P_5$ ), not characterized physically and chemically, non-volatilized intermediates ( $B_1, B_2$ ), and products  $R_1\text{--}R_3$  with their reaction coefficients  $f_1\text{--}f_{10}$ . The process was simulated using the fourth-order Runge-Kutta method.

Noteworthy is that in the work [13] the models proposed in papers [11, 12] were, besides the Yugoslavian oil shales, applied for description of the decomposition kinetics of Estonian oil shale. The apparent kinetic constants,  $E$  and  $A$ , for kukersite derived from TGA curves were 140–150 kJ/mol and  $3.53E + 09\text{--}1.77E + 10 \text{ min}^{-1}$ , and derived from d.s.c. data – 182 kJ/mol and  $1.0E + 14 \text{ min}^{-1}$ . The decomposition characteristics of kukersite established by the multi-step model are given in Table 1.

Table 1. Multi-Step Model Parameters for Kukersite [13]

Reaction	$A, \text{min}^{-1}$	$E, \text{kJ/mol}$							
$K \rightarrow f_1B_1 + f_2P_1$	$2E + 15$	200							
$f_1B_1 \rightarrow f_3B_2 + f_4P_2$	$1.06E + 14$	200							
$f_3B_2 \rightarrow f_5R_1 + f_6P_3$	44.7	42							
$B \rightarrow f_7R_2 + f_8P_4$	44.7	41							
$f_3B_2 \rightarrow f_7R_2 + f_8P_4$	44.7	41							
$f_5R_1 \rightarrow f_9R_3 + f_{10}P_5$	$3E + 05$	91							
$f_7R_2 \rightarrow f_9R_3 + f_{10}P_5$	$3E + 05$	91							
Reaction coefficients									
$f_1$	$f_2$	$f_3$	$f_4$	$f_5$	$f_6$	$f_7$	$f_8$	$f_9$	$f_{10}$
0.84	0.16	0.10	0.90	0.12	0.88	0.12	0.88	0.80	0.20

During the last twenty years there have been a number of more or less satisfactory approaches for modeling the pyrolysis kinetics of shales from different deposits.

Thermal behavior of Jordan oil shale has been studied by Haddadin *et al.* [14, 15] on the basis of isothermal and non-isothermal weight loss using TGA, and by Kraisha [16] under rapid heating conditions in a flash pyrolysis

unit. The TGA curves exhibited two endothermic peaks: s.c. softening (molecular rearrangements) and volatilization whose rate characteristics were found from the relationship

$$\log(d\alpha/dT)/(1 - \alpha)^n = \log A/b - E/(2.303RT) \quad (4)$$

where  $T$  was temperature related to time  $t$ ;  
 $n$  – reaction order.

The second endotherm gave by the least square fit of Equation (4) for the first-order kinetics of the untreated shale decomposition  $E = 79.6$  kJ/mol. and  $\log A = 5.2$ . Flash pyrolysis gave for Sultani and El Lajjun oil shales the activation energies 68.9 and 52.7 kJ/mol, and frequency factors 311.3 and 31.5 s<sup>-1</sup>, respectively.

The pyrolysis kinetics of some Australian oil shales was studied in a small stainless steel reactor (5 mm i.d. × 200 mm long). The pyrolysis products were detected by gas chromatographic analysis, mass spectrometry or H<sup>1</sup>n.m.r. [17–19]. The close agreement of experimental data with an empirical first-order kinetic model was obtained assuming the kerogen being composed of two discrete fractions ( $F_1$  and  $F_2$ ) with independent pyrolysis behavior

$$Y = F_1\{1 - \exp[-A_1 \exp(-B_1/T)t]\} + F_2\{1 - \exp[-A_2 \exp(-B_2/T)t]\} \quad (5)$$

where  $Y$  was the fraction of the residual volatiles;

$A_1$ ,  $B_1$ ,  $A_2$ ,  $B_2$ ,  $F_1$  and  $F_2$  were the coefficients used to fit the experimental values of  $Y$ ,  $T$  and  $t$  with Equation (5).

The values computed ranged as follows:

$$\begin{aligned} A_1 &= 6.0E + 12 - 1.5E + 22; B_1 = 25370 - 38000; \\ A_2 &= 8.4E + 10 - 1.5E + 25 \text{ s}^{-1}; B_2 = 23300 - 44000; \\ F_1 &= 0.5 - 1; F_2 = 0 - 0.5. \end{aligned}$$

Yang and Sohn [20] have described the kinetics of non-isothermal retorting of shales from different provinces of China by an overall first-order equation

$$\ln[-\beta \ln(1 - w/w_0)/RT^2] - \ln(1 - 2RT/E) = \ln(A/E) - E/RT \quad (6)$$

where  $w$  and  $w_0$  were the weight of oil evolved up to time  $t$  and the total weight of oil evolved during the process.

The values of  $A$  and  $E$  were estimated by repeated application of least-squares fit of Equation (6) to the experimental data. For this aim, at first an approximate value of  $E$  was applied in the left-hand side of Equation (6) to obtain  $-E/R$  from the slope and  $A/E$  from the intercept. The value of  $E$  found was then used in the left-hand side successively until no improvement in the value of  $E$  took place.

On the basis of TGA data Li and Yue [21] have developed a model for the kinetics of Chinese oil shale pyrolysis consisting of eleven parallel first-order reactions with the hypothetical activation energies from 80–280 kJ/mol. The share of each reaction ( $F_1$ – $F_{11}$ ) and the values of pre-exponential factors ( $A_1$ – $A_{11}$ ) as constants were computed using Monte Carlo method. As an interesting fact, the kinetic constants of the eleven hypothetical reactions gave a linear dependence of  $\ln A$  on  $E$  with regression coefficients characteristic to the shales (Fushun, Maoming and Huangxian) studied. In the paper [22] Li and Yue compared and discussed different models for determination of kinetic parameters from TGA data for pyrolysis of Fushun and Maoming oil shales. It was demonstrated that the overall differential model

$$\ln[\mathrm{d}\alpha/\mathrm{d}t(1 - \alpha)] = \ln(A/b) - E/RT \quad (7)$$

and the approximate integration model

$$\ln\{-\ln[(1 - \alpha)(E + 2RT)]/T^2\} = \ln(AR/b) - E/RT \quad (8)$$

gave lower results than Friedman procedure, the maximum rate method, and the parallel first-order method. Among the calculation methods tested the parallel model was suggested the most reasonable. The model assumed that the oil shale pyrolysis consisted of six parallel reactions with activation energies 80–280 kJ/mol. The main apparent energy of pyrolysis reactions was found to be in the ranges from 120 to 240 kJ/mol, and the values of  $A$  for Fushun and Maoming oil shales – in the ranges  $2.75\mathrm{E} + 06$ – $1.34\mathrm{E} + 16$  and  $1.28\mathrm{E} + 07$ – $5.21\mathrm{E} + 15 \mathrm{s}^{-1}$ .

The studies of Ballice [23] and Dogan [24] showed that a modification of the integral model expressed as the plot of  $\{-\ln[-\ln(1 - \alpha)]T^2\}$  vs.  $1/T$  did not represent a straight line for every Turkish oil shale. When a single kinetic expression was found to be valid for Beypazari oil shale, two parallel first-order expressions – pyrolysis of kerogen and bitumen – were suggested for Seyitömer and Himmetoğlu shales. At that, the values of activation energy found varied between 12 and 40 kJ/mol, depending on the shale and temperature interval.

Using TGA under non-isothermal conditions, Torrente and Galan [25] have estimated the values of  $E$  and  $A$  167 kJ/mol and  $2.16\mathrm{E} + 09 \mathrm{s}^{-1}$ , and under isothermal conditions 150 kJ/mol and  $2.11\mathrm{E} + 08 \mathrm{s}^{-1}$  for Spanish oil shale.

In all the works cited above [1–25] the pyrolysis kinetics was studied in open-air systems under non-isothermal conditions with constant heating rate, or under isothermal conditions. In these conditions the oil yield increased in time up to a constant level depending on the oil shale type and temperature. On the contrary, when pyrolysis is conducted in a closed vessel, a maximum occurs in the yield of liquid products.

Recently a simple step-by-step integral model was published [26] to describe the co-effects of time and temperature on the overall yields of oil, gas, and semicoke at pyrolysis of polyethylene in an autoclave under non-linear increase of temperature.

In this paper, the kinetic model proposed in [26] is modified and represented in the differential form. The model developed is applied for an approximate description of the transitions in time of the total gaseous, liquid and solid phases occurring at kukersite pyrolysis in autoclaves under non-linear increase of temperature.

## Experimental

In all the experiments 4.0 g of powdered and dried Estonian oil shale (kukersite) consisting of 51.4% organic matter (kerogen) were pyrolysed in micro-autoclaves (constant volume 20 ml). The autoclaves were weighed and placed into a muffle oven at three nominal temperatures (420, 450 and 500 °C). After 20–180 minutes the autoclaves were cooled and opened at room temperature. The mass of gas formed was determined by the weight loss after discharging. The liquid product (water + thermobitumen + oil) was extracted with hexane and tetrahydrofurane. The mass of the liquid product formed was found subtracting the mass of gas and dried solid residue from the initial mass of oil shale.

## Results and Discussion

The experimentally established time-dependencies of the yields of the products in grams per gram oil shale (Table 2) agree with the previous results [27]. The experimental points in grams per gram kerogen, and the corresponding interpolated curves used for estimation of the changes during short intervals are depicted in Fig. 1.

The results obtained demonstrate that pyrolysis does not start immediately after the autoclave has been placed into the oven. Obviously, the initial matter should achieve a certain temperature to initiate its thermal destruction. Noteworthy is that, differently from the previous works under open air conditions where the first products were, according to Aarna, gases, water and thereafter thermobitumen [2–4, 6], and according to Zakharov – oil [8, 9], in autoclaves under the conditions studied the formation of gas and liquid phases from kukersite starts practically simultaneously.

Basing on the scheme proposed by Aarna, at the first stage of pyrolysis the total liquid phase (water + thermobitumen + oil) should evolve from kerogen, and gas from the two products – from kerogen and from the liquid phase formed. At the next stage when kerogen is exhausted, the liquid phase should decrease due to the secondary gas and coke formation in the

autoclave. So, kinetics of the first period can be approximately described as a process consisting of three consequent-parallel reactions, and that of the second period – as a system of two parallel reactions. The according scheme is depicted in Fig. 2.

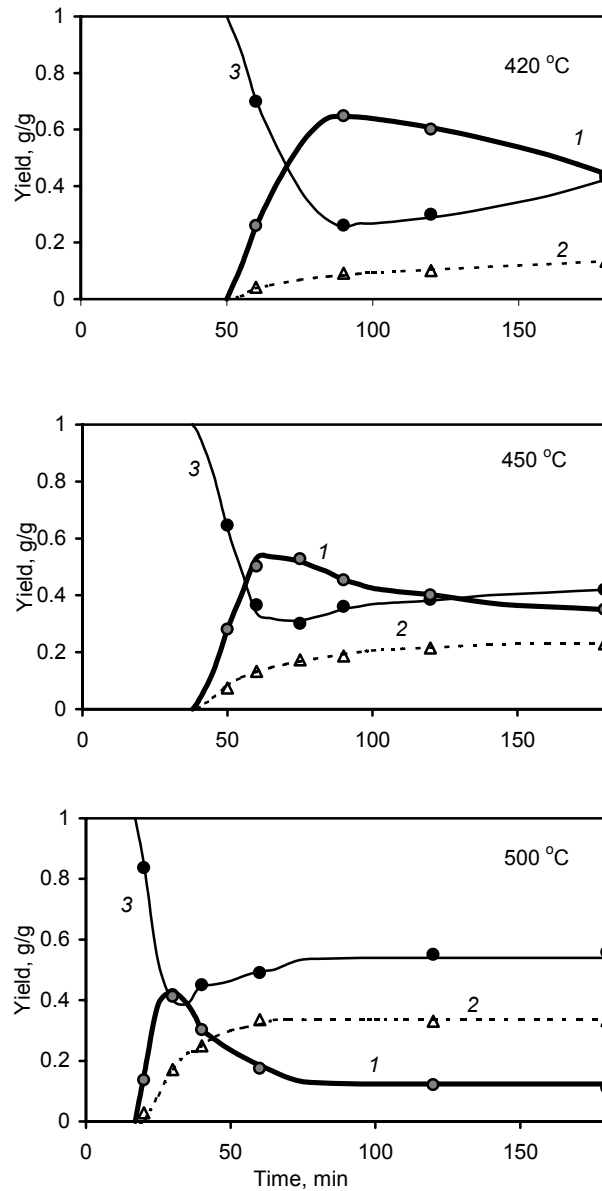


Fig. 1. Yields of the pyrolysis products from kerogen at different nominal temperatures: 1 – liquid product, 2 – gas, 3 – solid residue. Points experimental, curves interpolated

**Table 2. Yields of the Pyrolysis Products from Kukersite, %**

Time, min	Solid residue	Liquid product	Gas
Nominal temperature 420 °C			
60	84.55	13.31	2.14
90	61.96	33.31	4.73
120	63.99	30.84	5.17
180	70.60	22.51	6.89
Nominal temperature 450 °C			
50	81.81	14.39	3.80
60	67.39	25.80	6.80
75	64.01	27.09	8.90
90	67.10	23.28	9.61
120	68.37	20.61	11.02
180	70.19	17.99	11.82
Nominal temperature 500 °C			
20	91.57	6.99	1.44
30	70.05	21.18	8.77
40	71.68	15.52	12.80
60	73.79	8.94	17.27
120	76.87	6.17	16.96
180	82.77	0.11	17.12

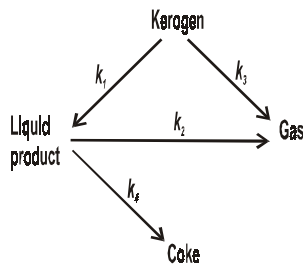


Fig. 2. Simplified scheme of kerogen pyrolysis

### Prediction of the Pyrolysis Current Temperature

Figure 3 depicts the time-dependencies of the kukersite temperature in the autoclaves recorded at oven temperatures 420, 450 and 500 °C.

The current temperature of a reaction mix in an autoclave ( $T_t$ ) at time  $t$  after being placed from room temperature ( $T_{room}$ ) into an oven with nominal temperature ( $T_{max}$ ) is fixed by the relationship [28, 29]

$$(T_{max} - T_t)/(T_{max} - T_{room}) = \exp(-\gamma Ft/cM) \quad (9)$$

where  $\gamma$  is total heat transfer coefficient;

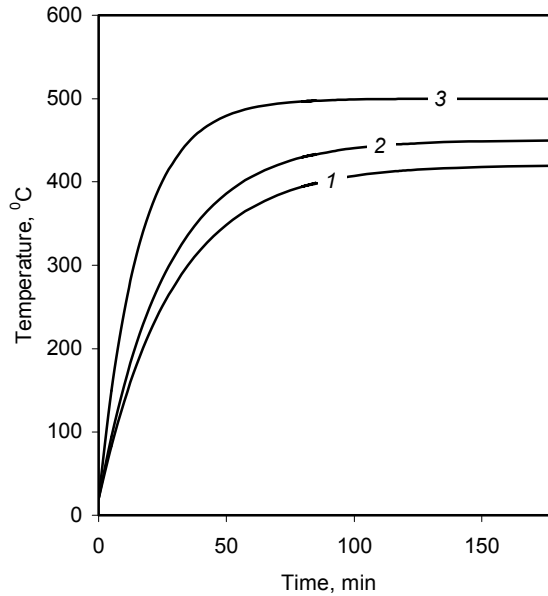
$F$  – total surface area of the autoclave;

$c$  – specific heat of the autoclave material (stainless steel);

$M$  – mass of the autoclave.



Fig. 3. Time-dependence of the reaction temperature at different nominal temperatures, °C: 1 – 420, 2 – 450, 3 – 500



In this work, the specifics of an autoclave in Equation (9) were brought together as its heating rate characteristic

$$\beta = \gamma F / cM \quad (10)$$

The value of  $\beta$  was found as the slope of the linear time-dependence of the function obtained taking logarithms from Equation (9) as follows:

$$\ln[(T_{max} - T_{room}) / (T_{max} - T_t)] = \beta t \quad (11)$$

Introducing the data presented in Fig. 3 into Equation (11) proves linearity of the graphs for all the three nominal temperatures tested. Particularly, the heating characteristic was not constant but the values obtained at temperatures 420, 450 and 500 °C, were 0.0344, 0.0381 and 0.0630  $\text{min}^{-1}$ , respectively. The increase in  $\beta$  with  $T_{max}$  was approximated to the regression

$$\beta = 9.45[(T - 20)/1000]^2 - 8.673(T - 20)/1000 + 2.020 \quad (12)$$

So, the current temperature of the reaction mix at any nominal temperature can be predicted introducing the value of  $\beta$  found by Equation (12) into Equation (13) as follows:

$$T_t = T_{max} - (T_{max} - T_{room}) \exp(-\beta t) \quad (13)$$

### Kinetic Equations

In this work, the thermal decomposition of oil shale according to the scheme in Fig. 2 is modeled as a combination of first-order kinetic equations for the sum of short-interval steps during which the current temperatures can be approximated to a constant mean value, and the current concentrations of the products can be approximated to their mean values over the interval.

Therefore, it is possible to describe the pyrolysis kinetics at any interval by simple relationships as follows:

- rate of OM decomposition

$$-(x_{0,n} - x_{0,n-1})/(t_n - t_{n-1}) = (k_1 + k_3)/[(x_{0,n-1} + x_{0,n})/2 - x_{0,\min}] \quad (14)$$

- rate of liquid phase formation

$$\begin{aligned} & (x_{1,n} - x_{0,n-1})/(t_n - t_{n-1}) = \\ & = k_1[(x_{0,n-1} + x_{0,n})/2 - x_{0,\min}] - (k_2 + k_4)(x_{1,n-1} + x_{1,n})/2 \end{aligned} \quad (15)$$

- rate of liquid phase decomposition at cracking

$$-(x_{1,n} - x_{0,n-1})/(t_n - t_{n-1}) = (k_2 + k_4)[(x_{1,n-1} + x_{1,n})/2 - x_{1,\infty}] \quad (16)$$

- rate of gas formation:  
in the stage of OM pyrolysis

$$(x_{2,n} - x_{2,n-1})/(t_n - t_{n-1}) = k_3[(x_{0,n-1} + x_{0,n})/2 - x_{0,\min}] + k_2(x_{1,n-1} + x_{1,n})/2 \quad (17)$$

and in the cracking stage

$$(x_{2,n} - x_{2,n-1})/(t_n - t_{n-1}) = k_2[(x_{1,n-1} + x_{1,n})/2 - x_{1,\infty}] \quad (18)$$

- rate of coke formation

$$(x_{3,n} - x_{3,n-1})/(t_n - t_{n-1}) = k_4[(x_{1,n-1} + x_{1,n})/2 - x_{1,\infty}] \quad (19)$$

where  $x_i$  is the current yield;

$k_i$  – rate coefficient;

index  $i$  shows the corresponding product: 0 – initial matter, 1 – liquid phase, 2 – gas, 3 – coke (look Fig. 2).

### Estimation of Kinetic Constants

First, the values of apparent kinetic rate coefficients at the cracking stage for coke and gas formation in five minutes intervals were calculated using the data from Fig. 1 and the modifications of Equation (13)–(19) as follows:

$$k_4 = (x_{3,n} - x_{3,n-1})/\{(t_n - t_{n-1})[(x_{1,n-1} + x_{1,n})/2 - x_{1,\infty}]\} \quad (20)$$

$$k_2 = (x_{2,n} - x_{2,n-1}) / \{(t_n - t_{n-1})[(x_{1,n-1} + x_{1,n})/2 - x_{1,\infty}]\} \quad (21)$$

Thereafter, regression coefficients for the Arrhenius plot

$$\ln k_2 = a_2 - b_2/T \quad (22)$$

were estimated for formation of gas from the liquid product (Fig. 4, curve 2).

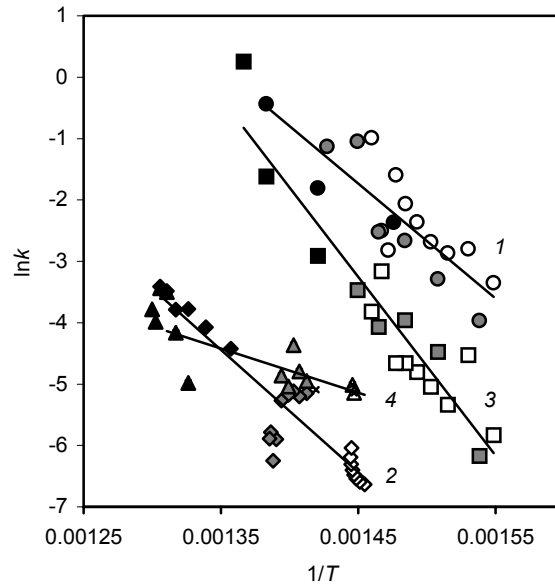


Fig. 4. Arrhenius plot of the apparent kinetic constants for different steps of pyrolysis at nominal temperatures, °C (420 – no fill, 450 – gray, 500 – black): 1 – formation of liquid product from kerogen, 2 – formation of gas from liquid product, 3 – formation of gas from kerogen, 4 – formation of semicoke from liquid product

Then, by means of  $a_2$  and  $b_2$  found the values of  $k_2$  were calculated for the short intervals of the liquid product destruction in the first stage. The corresponding values of  $k_3$  were calculated after replacements in Equation (17) as follows:

$$k_3 = [(x_{2,n} - x_{2,n-1}) / (t_n - t_{n-1}) - k_2(x_{1,n-1} + x_{1,n})/2] / [(x_{0,n-1} + x_{0,n})/2 - x_{0,\min}] \quad (23)$$

The values of  $k_1$  were calculated by means of the values of  $k_3$  found after replacements in Equation (14) as follows:

$$k_1 = -(x_{0,n} - x_{0,n-1}) / \{(t_n - t_{n-1})[(x_{0,n-1} + x_{0,n})/2 - x_{0,\min}]\} - k_3 \quad (24)$$

The Arrhenius plots of the rate coefficients vs.  $1/T_i$  obtained for each reaction under all the three nominal temperatures (see Fig. 4) show fairly

linear relationships. So, the scheme describing kinetics of the formation of different physical overall phases by the parallel-consequent reactions would be quite relevant for an approximate prediction of kukersite pyrolysis in autoclaves. The values of the corresponding apparent kinetic constants found by means of Fig. 4 are collected in Table 3.

**Table 3. Apparent Kinetic Constants for Kerogen Pyrolysis**

	$k_1$	$k_2$	$k_3$	$k_4$
$A$ , 1/min	1.13E+11	6.15E+09	2.15E+18	194
$E$ , kJ/mol	156	166	260	59.7

The results obtained demonstrate a substantial difference between the kinetic characteristics for gas formation from liquid phase ( $k_2$ ) and kerogen ( $k_3$ ), when at pyrolysis of polyethylene [26] the curves for gas formation from oil and melted initial polyethylene practically coincided.

As an intriguing fact, all the kinetic constants of different reactions at pyrolysis of kukersite found in this work using autoclaves, and in the works of others found using different open air equipments and mathematical models, can be approximated to a linear plot  $\ln A = a + bE$  (Fig. 5). Furthermore, when for kukersite,  $a$  is  $-3.26$  (min) and  $b$  is  $0.179$ , for Chinese Fushun, Maoming and Huangxian oil shales the kinetic constants calculated assuming eleven parallel hypothetical reactions gave the values of  $a$   $-2.01$ ,  $-1.13$  and  $-0.913$  (min), and  $b$   $0.1695$ ,  $0.1659$  and  $0.1656$ , respectively [21]. The kinetic constants estimated for pyrolysis of polyethylene in autoclaves [26] gave the value of  $a$   $0.318$  (min) and of  $b$   $0.138$ .

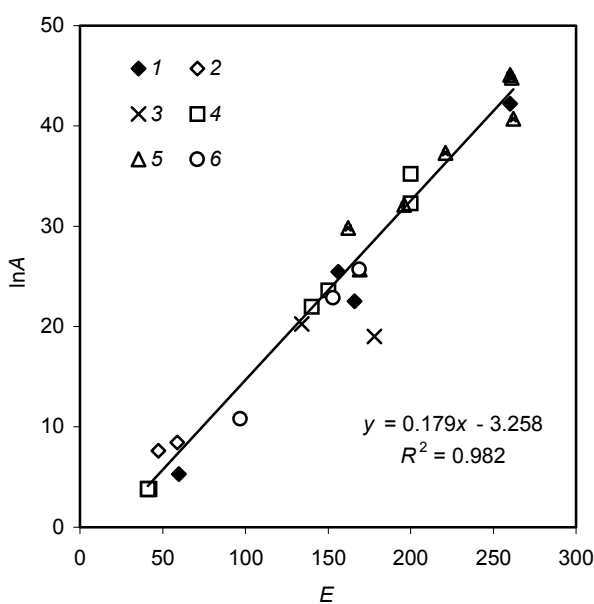


*Fig. 5. Plot of  $\ln A$  versus  $E$  for pyrolysis of kukersite compiled from the kinetic constants published in:*  
 1 – this work,  
 2 – [6],  
 3 – [9],  
 4 – [13],  
 5 – [10],  
 6 – gases in [9]

### Prediction of Current Concentrations

The experimental curves in Fig. 1 evidence that the initial kerogen cannot be totally exhausted at pyrolysis, and the yield of liquid products decreases to a limit value at cracking. At that, the higher the nominal temperature, the higher the minimum concentration of OM ( $x_{0,\min}$ ), and the lower the equilibrium concentration of the liquid products remained ( $x_{1,\infty}$ ).

On the basis of the experimental results (see Fig. 1) the dependencies of  $x_{0,\min}$  and  $x_{1,\infty}$  on the nominal temperature ( $^{\circ}\text{C}$ ) were approximated to the linear regressions

$$x_{0,\min} = 1.010 - 0.00180T_{\max} \quad (25)$$

$$x_{1,\infty} = -0.472 + 0.00170T_{\max} \quad (26)$$

It is clear that the coefficients in Equations (25) and (26), depending mainly on the gas pressure of the equilibrium processes, are valid only for the mass of kerogen in the autoclave applied ( $200 \text{ g/dm}^3$ ).

For predicting the yields of the products the following scheme was applied:

- 1) the current temperatures were calculated after every five minutes by Equations (12) and (13)
- 2) the corresponding values of rate coefficients were calculated using the Arrhenius relationship and constants given in Table 3
- 3) the yields of the products corresponding to time and temperature were calculated using the relationships deduced from Equations (14)–(19) as follows:

$$\bullet \quad x_{0,n} = \{x_{0,n-1}[2 - (k_1 + k_3)(t_n - t_{n-1})] + 2x_{0,\min}(k_1 + k_3)(t_n - t_{n-1})\} / [2 + (k_1 + k_3)(t_n - t_{n-1})] \quad (27)$$

for the stage of OM pyrolysis:

$$\bullet \quad x_{1,n} = \{[2 - (k_2 + k_4)(t_n - t_{n-1})]x_{1,n-1} + k_1(x_{0,n-1} + x_{0,n})(t_n - t_{n-1})\} / [2 + (k_2 + k_4)(t_n - t_{n-1})] \quad (28)$$

$$\bullet \quad x_{2,n} = x_{2,n-1} + [k_2(x_{1,n-1} + x_{1,n}) + k_3(x_{0,n-1} + x_{0,n})](t_n - t_{n-1})/2 \quad (29)$$

and for the stage of cracking:

$$\bullet \quad x_{1,n} = \{[2 - (k_2 + k_4)(t_n - t_{n-1})]x_{1,n-1} + 2(k_2 + k_4)(t_n - t_{n-1})x_{1,\infty}\} / [2 + (k_2 + k_4)(t_n - t_{n-1})] \quad (30)$$

$$\bullet \quad x_{2,n} = x_{2,n-1} + k_2[(x_{1,n-1} + x_{1,n})/2 - x_{1,\infty}](t_n - t_{n-1}) \quad (31)$$

$$\bullet \quad x_{3,n} = x_{3,n-1} + k_4[(x_{1,n-1} + x_{1,n})/2 - x_{1,\infty}](t_n - t_{n-1}) \quad (32)$$

Comparison of the predicted by Equations (25)–(32) yields with the experimental data (Fig. 6) shows that the simple model proposed could be applied for an approximate prediction of transformations of the overall phases at kukersite pyrolysis in the autoclaves.

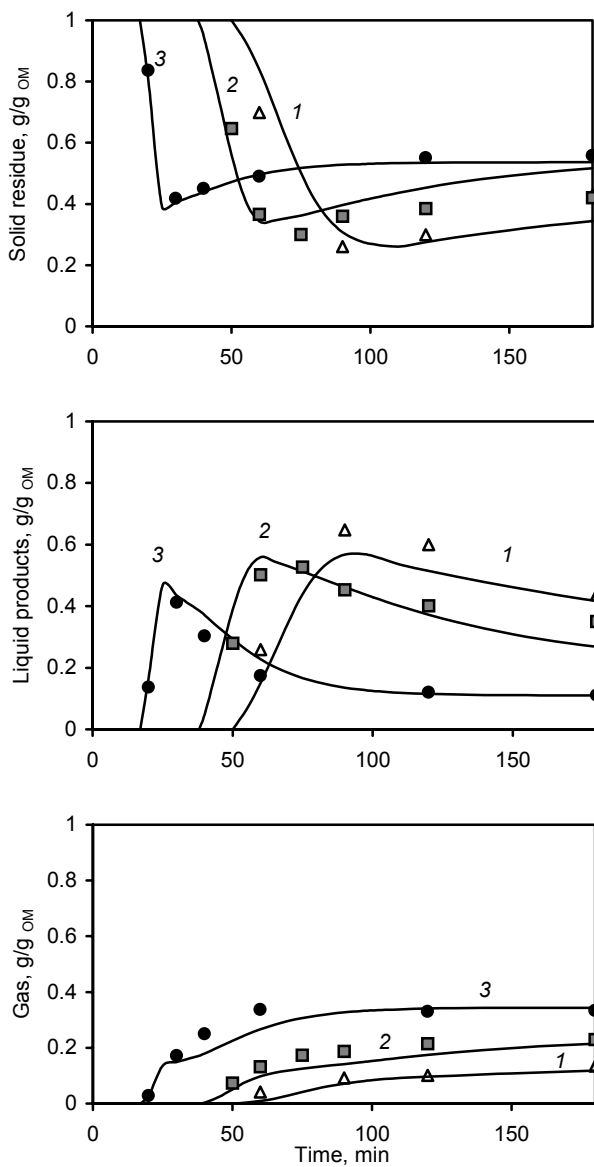


Fig. 6. Comparison of the predicted and experimental yields of the pyrolysis products obtained at different nominal temperatures, °C: 1 – 420, 2 – 450, 3 – 500. Points experimental, curves calculated

## Conclusions

A simple step-by-step model has been deduced for an approximate description of kukersite pyrolysis kinetics in an autoclave under non-linear increase of temperature. The values of the apparent rate coefficients and their temperature dependencies have been estimated for the thermal decomposition of kerogen into gaseous and liquid products, and the secondary cracking of the liquid product into gas and solid residue. A linear relationship between the Arrhenius kinetic constants  $\ln A-E$  was revealed using the data ( $n = 24$ ) published in different studies about pyrolysis of kukersite.

## Acknowledgements

The authors thank Estonian Science Foundation for the financial support (grants No. 5357 and No. 5359).

## REFERENCES

1. *Hissin, Y. I.* Thermal Decomposition of Oil Shale. – *Gostoptechizdat*, 1948 [in Russian].
2. *Aarna, A.* Isothermal destruction of Baltic oil shale // Proceedings of Tallinn Polytechnic Institute. 1954. Series A. No. 57. P. 32–34 [in Russian].
3. *Aarna, A.* About isothermal destruction of Baltic oil shale // *J. Appl. Chem.* 1955. Vol. 28. P. 1138–1142 [in Russian].
4. *Aarna, A.* About kinetics of thermal destruction of Baltic oil shale // *J. Appl. Chem.* 1956. Vol. 29. P. 606–610 [in Russian].
5. *Kollerov, D. K.* Rate of thermal destruction of organic matter from oil shales // *Chemistry and Technology of Fuels* // 1956. No. 10. P. 55–62 [in Russian].
6. *Aarna, A., Lippmaa, E.* Thermal destruction of oil shale-kukersite // Proceedings of Tallinn Polytechnic Institute. Series A. 1958. No. 97. P.3–27 [in Russian].
7. Thermal Destruction of Shale-Kukersite / M.Y. Gubergrits (ed.). – Tallinn : *Valgus*, 1966. P. 27–32 [in Russian].
8. *Zakharov, V. Yu., Shchuchkin, J. A.* Kinetics of evolution of individual gases in the course of shale thermal decomposition. 2. Kinetic parameters // *J. Therm. Anal.* 1986. Vol. 31. No. 4. P. 805–812.
9. *Zakharov, V. Yu., Rundygin, Yu. A., Shchuchkin, I. A.* The kinetics of oil shale thermal decomposition // *Oil Shale*. 1988. Vol. 5, No. 1. P. 74–80 [in Russian, with English summary].
10. *Kundel, H., Petaja, L.* Kinetics of thermal destruction of oil shale Kukersite // Problems of creation of huge generators for semicoking of oil shales / Collection of scientific works. Institute of Oil Shale Research. 1991 Vol. 25. P. 3–17 [in Russian].

11. Skala, D., Kopsch, H., Sokić, M., Neumann, H.-J., Jovanović, J. Modelling and simulation of oil shale pyrolysis // *Fuel*. 1989. Vol. 68. P. 168–174.
12. Skala, D., Kopsch, H., Sokić, M., Neumann, H.-J., Jovanović, J. Thermogravimetrically and differential scanning calorimetrically derived kinetics of oil shale pyrolysis // *Fuel*. 1987. Vol. 66. P. 1185–1191.
13. Skala, D., Kopsch, H., Sokić, M., Neumann, H.-J., Jovanović, J. Kinetics and modelling of oil shale pyrolysis // *Fuel*. 1990. Vol. 69. P. 490–496.
14. Haddadin, R. H., Tawarah K, M. DTA derived kinetics of Jordan oil shale // *Fuel*. 1980. Vol. 59. P. 539–543.
15. Haddadin, R. H. A kinetic and mechanistic comparison for Jordan oil shale pyrolysis and dissolution // *Fuel Processing Technology*. 1982. Vol. 6. P. 235–243.
16. Kraisha, Y. H. Flash pyrolysis of oil shales in a fluidized bed reactor // *Energy Conversion & Management*. 2000. Vol. 41. P. 1729–1739.
17. Ekstrom, A., Callaghan, G. The pyrolysis kinetics of some Australian oil shales // *Fuel*. 1987. Vol. 66. P. 331–337.
18. Wall, G. C., Smith, S. J. C. Kinetics of production of individual products from the isothermal pyrolysis of seven Australian oil shales // *Fuel*. 1987. Vol. 66. P. 345–349.
19. Parks, T. J., Lync, L. J., Webster, D. S. Pyrolysis model of Rundle oil shale from *in-situ* <sup>1</sup>H n.m.r. data // *Fuel*. 1987. Vol. 66. P. 338–344.
20. Yang, H. S., Sohn, H. Y. Kinetics of oil generation from oil shale from Lioing province of China // *Fuel*. 1984. Vol. 63. P. 1511–1514.
21. Li, S., Yue, C. Study of pyrolysis kinetics of oil shale. // *Fuel*. 2003. Vol. 82. P. 337–342.
22. Li, S., Yue, C. Study of different kinetic models for oil shale pyrolysis // *Fuel Processing Technology*. 2004. Vol. 85. P. 51–61.
23. Ballice, L., Yüksel, M., Saglam, M., Schulz, H., Hanoglu, C. Application of infrared spectroscopy to the classification of kerogen types and the thermogravimetrically derived pyrolysis kinetics of oil shale // *Fuel*. 1995. Vol. 74. P. 1618–1623.
24. Dogan, O. M., Uysal, B. Z. Non-isothermal pyrolysis kinetics of three Turkish oil shales // *Fuel*. 1996. Vol. 75. P. 1424–1428.
25. Torrente, M. C., Galan, M. A. Kinetics of the thermal decomposition of oil shale from Puertollano // *Fuel*. 2001. Vol. 80. P. 327–334.
26. Johannes, I., Tamvelius, H., Tiikma, L. A step-by-step model for pyrolysis kinetics of polyethylene in an autoclave under non-linear increase of temperature // *J. Anal. Appl. Pyrolysis*. 2004. Vol. 72. P. 113–119.
27. Tiikma, L., Prjadka, N., Luik, H. Co-pyrolysis of Estonian shales with low-density polyethylene // *Oil Shale*. 2004. Vol. 21. P. 75–85.
28. Holman, J. P. *Heat Transfer*. 4th ed. – New York, 1976. P. 98.
29. *Thermal-Physics. Measurements and Apparatus* / E. S. Platunov (ed.). – Maschine-Building, Leningrad, 1986 [in Russian].

*Presented by L. Mölder*

Received March 17, 2004